PERGAMON

Available online at www.sciencedirect.com

SCIENCE DIRECT®

Solid State Communications 127 (2003) 583–588

solid state communications

www.elsevier.com/locate/ssc

A novel method of fabricating porous silicon material: ultrasonically enhanced anodic electrochemical etching

Y. Liu[a], Z.H. Xiong[a], Y. Liu[a], S.H. Xu[a], X.B. Liu[a], X.M. Ding[a], X.Y. Hou[a,b,*]

[a]*Surface Physics Laboratory (National Key Laboratory), Fudan University, Shanghai 200433, People's Republic of China*
[b]*Surface Physics Laboratory (National Key Laboratory) and Institute of Advanced Materials and Technology, Fudan University, Shanghai 200433, People's Republic of China*

Received 14 February 2003; accepted 23 April 2003 by Z. Gan

Abstract

Ultrasonically enhanced anodic electrochemical etching is developed to fabricate luminescent porous silicon (PS) material. The samples prepared by the new etching method exhibit superior characteristics to those prepared by conventional direct current etching. By applying ultrasonically enhanced etching, PS microcavities with much higher quality factors can be fabricated. The improved quality induced by ultrasonic etching can be ascribed to increased rates of escape of hydrogen bubbles and other etched chemical species from the porous silicon pillars' surface. This process will cause the reaction between the etchant and the silicon wafer to proceed more rapidly along the vertical direction in the silicon pores than laterally.
© 2003 Elsevier Ltd. All rights reserved.

PACS: 82.45.Yz; 78.55.Mb; 43.35. + d

Keywords: A. Nanostructures; D. Optical properties; E. Ultrasonics

Since the report of room-temperature visible light emission from porous silicon (PS) [1,2], this easy-fabricating and low cost luminescent material has been drawing great interests [3–6] because of its potential applications in integrated optoelectronics fields. The most commonly used method of fabricating PS is direct current (DC) anodic electrochemical etching [1]. During the DC anodic etching process, the reaction product, silicon fluoride [7], tends to deposit at the pore tips. The H_2 bubbles are adsorbed at the surface of silicon pillars because of interfacial tension, blocking the silicon pores and leading to a reduction of HF concentration inside the pores [8]. Thus, the etching process will be slowed down. Meanwhile, the dissolved species will increase the resistance of silicon wafer and hence decrease the current density. This factor also slows down the etching rate. In 1996, a pulsed anodic etching method was developed in this lab, which carries out the anodic etching in an intermittent mode [9]. This etching method lets the chemical products diffuse from the silicon pores during the pause period of anodic current and is therefore superior compared to DC anodic etching [9,10]. However, the speed of natural diffusion of silicon fluoride and H_2 bubbles using pulsed anodic etching is still very slow.

In this work, an ultrasonically enhanced anodic electrochemical etching is developed to fabricate light-emitting PS material. Taking advantage of the ultrasonic press effect and acoustic cavitation [11], the diffusion of the dissolved species and H_2 bubbles from silicon pores can be accelerated. Scanning electron microscopy (SEM), atomic force microscopy (AFM) and photoluminescence (PL) investigations show that the PS material prepared by ultrasonic anodic etching has improved qualities in surface morphology, layer interface smoothness, etching efficiency and optical characteristic compared with the sample prepared by DC etching. Combination of the former pulsed anodic etching with ultrasonic anodic etching proves to be

* Corresponding author. Address: Surface Physics Laboratory (National Key Laboratory), Fudan University, Shanghai 200433, People's Republic of China. Fax: +86-651-04949.

E-mail address: xyhou@fudan.edu.cn (X.Y. Hou).

0038-1098/03/$ - see front matter © 2003 Elsevier Ltd. All rights reserved.
doi:10.1016/S0038-1098(03)00489-7

Table 1
The parameters of different etching methods for fabricating PS

Sample	Etching method	Current density (mA/cm^2)	Time (s)	Duty cycle
A	DC etching	50	180	/
B	Pulsed etching	50	360	1:2
C	Ultrasonic etching	50	180	/
D	Ultrasonic + pulsed etching	50	360	1:2

an efficient method to fabricate PS material, especially PS multilayer.

The substrate used was a (100)-oriented highly doped (0.01 Ω cm) p + -type silicon single crystal wafer. It was placed in a Teflon etching cell and etched in the dark with a HF (40%): C_2H_5OH (99%):H_2O = 1:1:2 (by volume) electrolyte solution. For comparison, we prepared a series of samples with four different etching methods: DC anodic etching, pulsed anodic etching, ultrasonic anodic etching and pulsed plus ultrasonic anodic etching. In this letter, four samples are presented and referred to as sample A, B, C and D, respectively. The etching parameters are listed in Table 1. Under the same etching current density, samples B and D, prepared by pulsed etching with duty cycle of 0.5, were given doubled non-electrochemical etching (pause of the etching) time for unifying absolute etching time with samples A and C. For details of pulsed anodic etching, see Refs. [9,10]. The ultrasonic wave frequency of the ultrasonic generator was 33 ± 3 kHz. After the etching process, all the samples were immediately rinsed by de-ionized water and dried.

The surface and cross-sectional structures were investigated with Philips XL 30 FEG Field Emission Scanning Electron Microscope (FESEM), the minimum resolution of which is 2 nm and acceleration voltage 0.2–30 kV. Analysis of surface morphology was carried out using the AFM component of a model of P_{47}-SPM-MDT Scanning Probe Microscope (SPM).

The PL spectra of the samples were measured using the 441.6 nm line of a He–Cd laser as the excitation source. The source of the reflection spectra was a 250 W tungsten halogen lamp; the signals were amplified by standard lock-in techniques, and detected by a photomultiplier.

Fig. 1 shows the surface SEM images of samples A, B, C

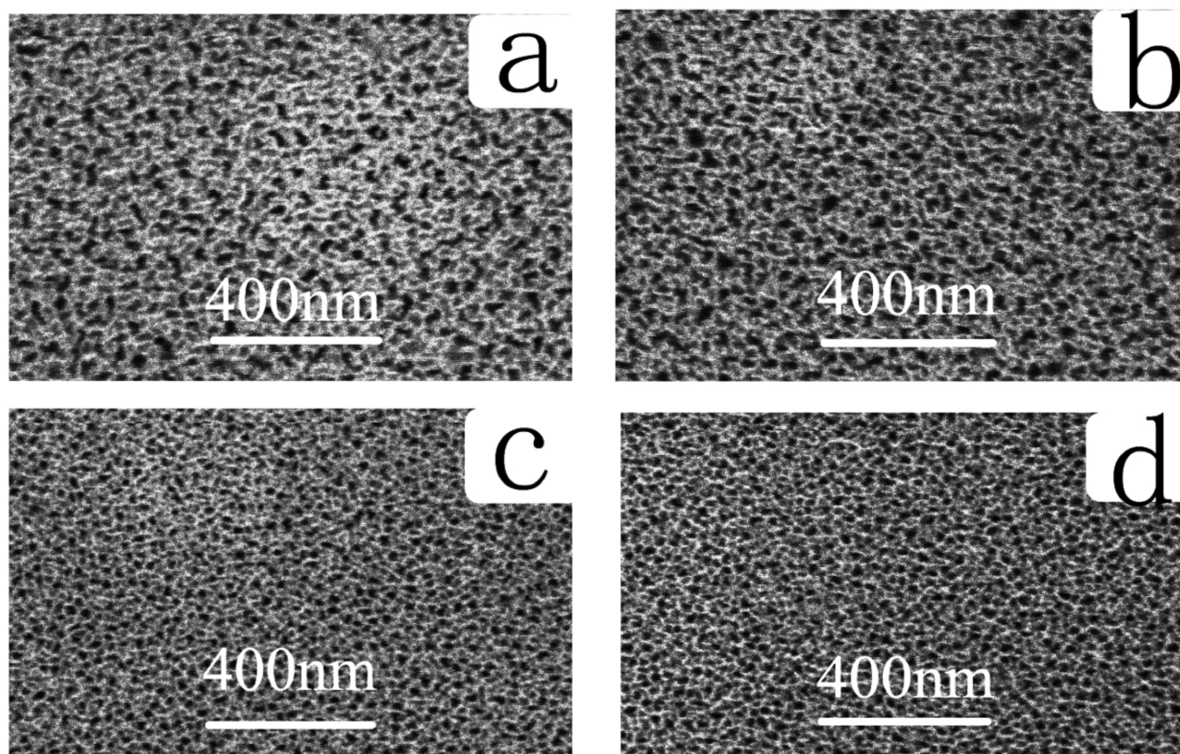

Fig. 1. Surface SEM micrographs of porous silicon samples fabricated by four different etching methods: (a) DC etching (sample A), (b) pulsed etching (sample B), (c) ultrasonic etching (sample C), and (d) ultrasonic plus pulsed etching (sample D).

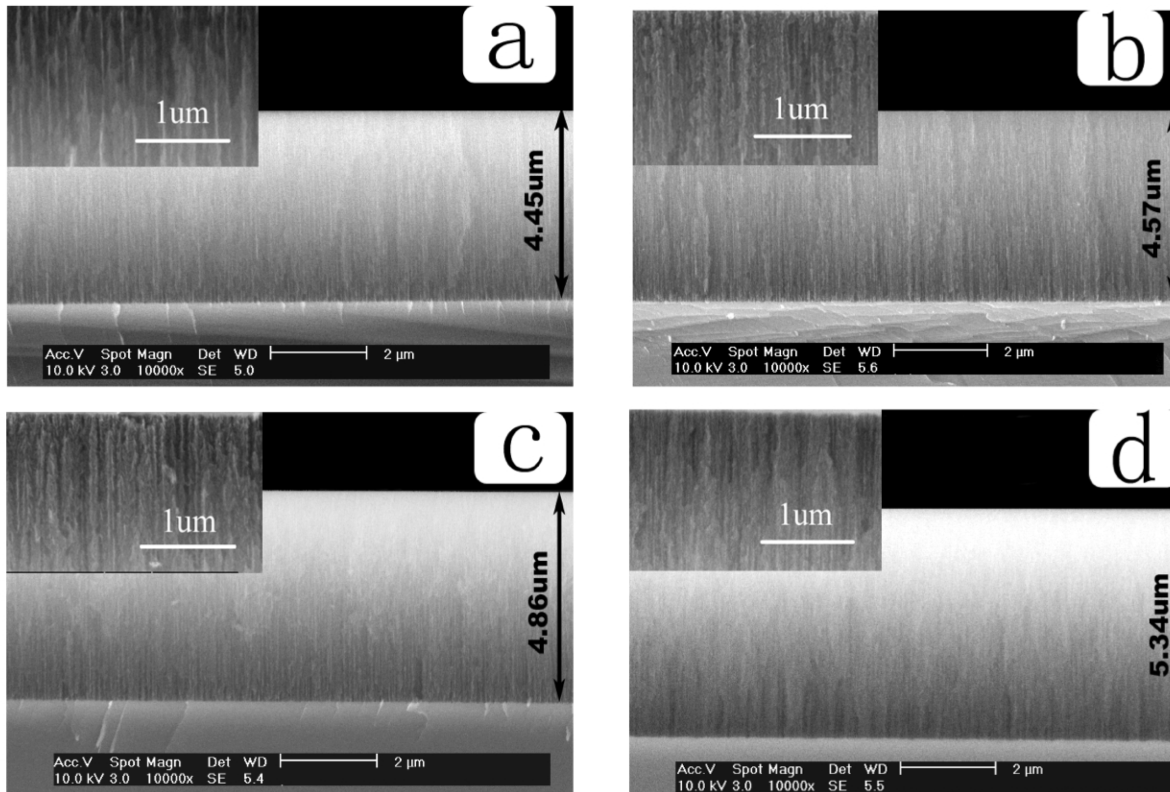

Fig. 2. Cross-sectional SEM micrographs of our four samples: (a) sample A, (b) sample B, (c) sample C, and (d) sample D. The four insets show the enlarged images of the four samples, respectively.

and D; the pores in the PS samples are seen as dark dots. Fig. 1(a) shows the pores of sample A distribute themselves randomly and are irregularly shaped. Most pores have large dimensions that seem to be joined by two or more smaller pores. The result of sample B is shown in Fig. 1(b). One can see from the image that the uniformity of PS pores has been slightly improved. AFM investigations, discussed below, show more direct evidence. Samples C and D, fabricated using ultrasonic wave, are shown in Fig. 1(c) and (d). The pore diameters are much smaller and the shapes are more circular than in samples A and B. More uniform distributions of homogeneous pores have appeared in Fig. 1(c) and (d). The mean area of surface pores in SEM images (Fig. 1(a)–(d)) reduces from 886 nm^2 for sample A, to 320 nm^2 for sample C and from 563 nm^2 for sample B to 191 nm^2 for sample D. In addition, when viewed by naked eye, the fresh-prepared samples B, C and D shine a uniform interference color while for sample A the color varies from the center to the edge. This is indirect evidence that samples B, C and D have uniform PS layer while sample A does not, which is further confirmed by PL spectra.

The cross-sectional SEM images of the four samples are shown in Fig. 2(a)–(d). The PS layer thickness of samples A, B, C and D are 4.45, 4.57, 4.86 and 5.34 μm, respectively. In the same effective etching time, two obvious conclusions can be obtained: (1) the PS layer thickness of samples prepared by ultrasonic etching (samples C and D) are larger than that of samples prepared by non-ultrasonic etching (samples A and B) and (2) the layer thickness of the samples prepared by pulsed etching are larger than those prepared by non-pulsed etching. The insets of Fig. 2 are enlarged images of the four samples. The silicon pores of sample D are the most continuous in the surface-normal direction and have both the most uniform distribution and the smallest diameters.

Considering the dielectric constant of PS is a function of its porosity, a Bragg reflector and PS multilayer structure can be constructed to manipulate the light transmission in PS multilayers [12]. Therefore, the surface and interface smoothness is one of the key factors determining optical characteristics of PS multilayer. Smoothness of the four samples was measured by AFM and is shown in Fig. 3. The most obvious phenomenon displayed in the micrograph is that the silicon pillar dimension increases from sample D to sample A while the uniformity decreases. The surface roughness root mean square (RMS) value for each of the four samples is 17.324 nm (sample A), 9.505 nm (sample B), 3.779 nm (sample C) and 2.430 nm (sample D).

The above surface and cross-sectional morphology studies of the samples indicate that, when fabricated using

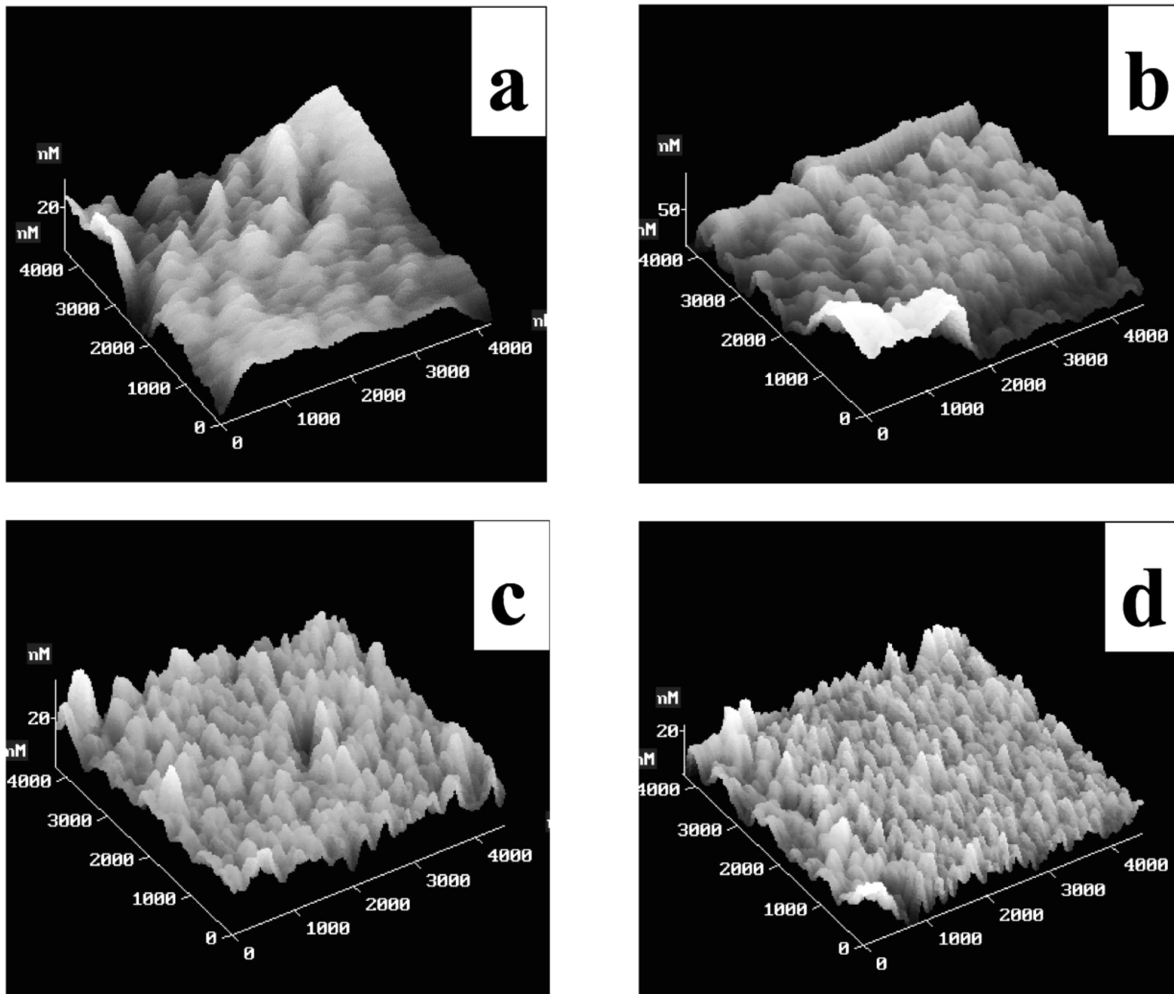

Fig. 3. AFM images of (a) sample A, (b) sample B, (c) sample C, and (d) sample D, with RMS of 17.324, 9.505, 3.779, and 2.43 nm, respectively.

ultrasonic anodic etching, a sample has a more uniform PS layer with smaller silicon pores and the etching efficiency is also higher than those prepared by other means. The reason is believed to be that when employing simply the DC etching method, the chemical reaction products will deposit at silicon pores, mostly at pore tips, and prevent the dissolution of silicon wafer, consequently enlarging the lateral etching. A lot of micro-bubbles will appear in the electrolyte solution when the ultrasonic wave acts on it. These bubbles will shrink and expand repeatedly with the variety of sound pressure and result in desorbing of the chemical products from silicon pillars. If the bubble is broken, an extreme high pressure will be produced. This pressure will bring the dissolved species out of the silicon pores. In addition, the other ultrasonic effects, such as vibration, will also speed up the diffusion of chemical products. All these reasons cause the chemical reaction to concentrate on the pore tips, thereby reducing the lateral etching and improving the uniformity and etching efficiency.

The light interference caused by up and down interfaces of PS single layer sample manifests itself as multiple peaks in the PL spectrum. From this, the information about interface smoothness can be obtained. Fig. 4 is the visible PL spectra of the four samples. Oscillating peaks appearing in PL spectra of samples B, C and D show that the layer smoothness of the three samples is better than that of sample A. According to film optics, the larger the amplitude of oscillating peaks, the better the smoothness of the PS films: sample D has the best quality smoothness yet sample A has the worst. Excellent optical characteristics depend on good sample construction; this is also shown by the PL enhancement seen from sample A to sample D. Referring to the theory of optical interference, the oscillating peaks are caused by the interference of different grades of emergent light, which is emitted by PS material and reflected by up

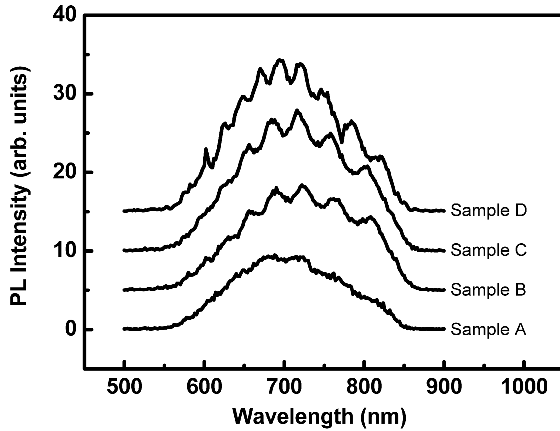

Fig. 4. PL spectra of samples A, B, C, and D in the visible region.

and down interfaces. Therefore, we have $2nd = k\lambda = (k-1)\lambda'$, where n is the refractive index of the PS layer, d is thickness (obtained in the former SEM images), k is the grade of light wave and λ, λ' are the different peak wavelengths for two adjacent peaks. The n is given by $n = \lambda\lambda'/(\lambda' - \lambda)2d$. From this we have calculated the refractive indexes of the four samples as 1.39 (sample A), 1.55 (sample B), 1.50 (sample C) and 1.71 (sample D), respectively. As known from previous work [1,7,13], high porosity, corresponding to low refractive index, is essential for efficient visible PL. Conversely, in our experiment, the sample with higher refractive index, prepared by ultrasonic etching, has a higher PL efficiency than those samples with lower refractive indices fabricated by conventional electrochemical etching. The efficient luminescence from this sample can be explained by its more homogeneous nanostructure.

For studying interface smoothness of PS multilayer further, the PS microcavities were fabricated. The full width at half maximum (FWHM) of the resonant PL peak from the PS microcavity can be regarded as a reflection of PS multilayer interface quality. Fig. 5(a) is the reflection and PL spectra of the PSM sample prepared by pulsed anodic etching. The PL peak is located at 680 nm with the FWHM of 8 nm, corresponding to a quality factor (Q) of 85 for the microcavity. The result of PS microcavity fabricated by ultrasonic anodic etching is shown in Fig. 5(b). The peak shifts to 794 nm and the FWHM decreases to less than 4 nm. It is considered that the narrowed PL peak in Fig. 5(b) is due to the increased PS layer smoothness and improved PS microcavity's modulation. The ultrasonic etching process wave makes all the PS microcavity layers thicker and with larger refractive index, which results in the modulation waveband of PS microcavity moving to long-wavelength region and resulting in red-shift of PL peak. The Q here values more than 200, much higher than previously reported [14]. These results lay a foundation for exploiting of PS devices, particularly in realizing PS laser. The spectral analysis of both PS single layer and PS microcavity

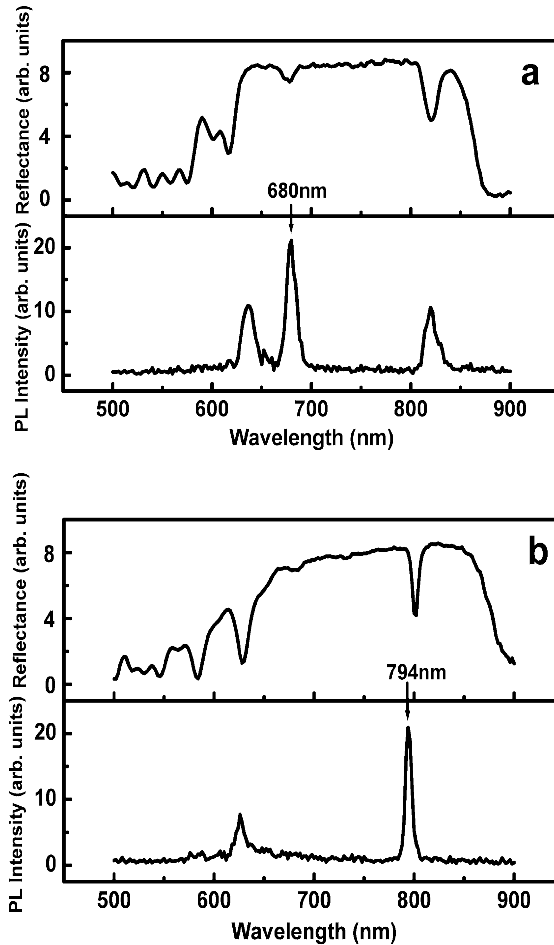

Fig. 5. Reflectance and PL spectra of porous silicon microcavities fabricated by pulsed etching (a) without ultrasonic wave and (b) with ultrasonic wave.

indicates that by employing the ultrasonic anodic etching method, the optical characteristic of PS materials can be greatly improved.

In summary, we have presented an ultrasonic anodic etching method for fabricating light-emitting PS material. Surface and cross-sectional SEM investigations reveal that when other etching parameters are constant, the ultrasonic etching creates a thicker and more uniform PS layer, with smaller silicon pores than DC etching and pulsed etching. AFM observations further confirm the improved structural properties, which can be explained by the PS formation mechanics, especially by ultrasonic cavitation. The studies of both PS single layer and PS microcavity show that ultrasonic etching optimizes the sample's optical characteristics. The best quality sample has been acquired by combining the ultrasonic etching with pulsed etching. This new etching method is an efficient technique to fabricate PS materials, especially PS multilayer, and opens a feasible way to realizing the application of PS materials.

Acknowledgements

This work was supported by the Chinese National Key Basic Research Special Fund (Grant No. 2001CB610408), the National Natural Science Foundation of China and the Shanghai Municipal Commission of Science and Technology. The authors also thank Edward Obbard for a critical checking of the manuscript.

References

[1] L.T. Canham, Appl. Phys. Lett. 57 (1990) 1046.
[2] V. Lehmann, U. Gösele, Appl. Phys. Lett. 58 (1991) 856.
[3] P.M. Fauchet, J. Lumin. 70 (1996) 294.
[4] A.G. Cullis, L.T. Canham, P.D.J. Calcott, J. Appl. Phys. 82 (1997) 909.
[5] L.T. Canham, A.G. Cullis, C. Pickering, O.D. Dosser, T.I. Cox, T.P. Lynch, Nature 368 (1994) 133.
[6] V. Pellegrini, F. Fuso, G. Lorenzi, M. Allegrini, A. Diligenti, A. Nannini, G. Pennelli, Appl. Phys. Lett. 67 (1995) 1084.
[7] O. Bisi, S. Ossicini, L. Pavesi, Surf. Sci. Rep. 38 (2000) 1.
[8] V. Lehmann, J. Eletroanal. Chem. 140 (1993) 2836.
[9] X.Y. Hou, H.L. Fan, L. Xu, F.L. Zhang, M.Q. Li, M.R. Yu, X. Wang, Appl. Phys. Lett. 68 (1996) 2323.
[10] Z.H. Xiong, L.S. Liao, X.M. Ding, S.H. Xu, Y. Liu, L.L. Gu, F.G. Tao, S.T. Lee, X.Y. Hou, Appl. Phys. A 74 (2002) 807.
[11] N. Feng, Ultrasonic Handbook, Nanking University Press, 1999.
[12] V. Pellegrini, A. Tredicucci, C. Mazzoleni, L. Pavesi, Phys. Rev. B 52 (1995) 14328.
[13] P.M. Fauchet, J. von Behren, Phys. Status Solidi B 204 (1997) R7.
[14] L. Pavesi, C. Mazzoleni, A. Tredicucci, V. Pellegrini, Appl. Phys. Lett. 67 (1995) 3280.